Available online at www.sciencedirect.com
SCIENCE DIRECT®
ELSEVIER
Catalysis Today 115 (2006) 179–185
CATALYSIS TODAY
www.elsevier.com/locate/cattod

Light alkanes CO_2 reforming to synthesis gas over Ni based catalysts

A. Olafsen [a], C. Daniel [b], Y. Schuurman [b], L.B. Råberg [c], U. Olsbye [c], C. Mirodatos [b,*]

[a] SINTEF Materials and Chemistry, P.O. Box 124 Blindern, Oslo N-0314, Norway
[b] Institut de Recherches sur la Catalyse, CNRS, 2 Avenue A. Einstein, 69626 Villeurbanne, France
[c] Department of Chemistry, Centre for Materials Science and Nanotechnology, University of Oslo, P.O. Box 1033 Blindern, Oslo N-0315, Norway

Abstract

The CO_2 reforming of methane and propane has been compared over two different Ni catalysts: one reference Ni/SiO_2 system and a Ni/Mg(Al)O hydrotalcite-derived catalyst, shown previously to display high catalytic stability for long term reforming. By combining the Tapered Element Oscillating Microbalance (TEOM), Temperature Programmed Hydrogenation (TPH), Transmission Electron Microscopy (TEM) and magnetic measurements, the formation of coke and its role on the catalyst activity has been investigated and compared for both hydrocarbons. It was found that Ni/SiO_2 and Ni/Mg(Al)O are both more active for methane reforming than for propane reforming. Coke formation is much more pronounced for propane than for methane over both catalysts. However, for both hydrocarbons a much faster carbon formation is observed over the Ni/SiO_2 catalyst than over the Ni/Mg(Al)O catalyst. The difference in the rates of coke formation for methane and propane is ascribed in the case of propane to partially dehydrogenated C_3 adspecies, which are good coke precursors. The superior stability of the hydrotalcite-derived catalyst is due to the strong interaction of the nickel phase with the support and the capacity of the support to activate CO_2 and channel oxygen to the nickel phase.

Keywords: Methane; Propane; TEOM; TPH; Magnetic measurements; Dry reforming; Coke formation

1. Introduction

Crude natural gas may contain in addition to methane ca. 10 vol.% of light alkanes (C_2–C_4) and up to 30 vol.% of CO_2. In order to convert it into syngas via reforming reactions without prior separation [in view of a Gas To Liquid (GTL) process], an overall understanding of both CH_4 and higher alkanes dry reforming mechanisms is required for developing catalysts with a high activity and selectivity towards CO and H_2, a high stability and a low selectivity to coke formation.

While numerous articles exist on the catalytic dry reforming of methane to synthesis gas, especially for nickel based catalysts [1], only few studies address the specificity of propane dry reforming, in general using supported noble metal catalysts (Rh, Ru) [2,3]. Recently, we extended our prior studies of methane dry reforming over Ni based catalysts towards propane dry reforming [4]. In this work, it is attempted to compare methane and propane CO_2 reforming on two types of Ni based systems; one reference Ni/SiO_2 system and a Ni/Mg(Al)O hydrotalcite-derived catalyst, which was shown previously to display high catalytic stability for a long term reforming period [4].

After comparing the catalytic stability for the two systems toward the two feed gases (methane and propane), it is attempted to understand the carbon deposition processes and the specific role of each carbon deposit for the catalytic cycle as well as for the ageing process. The Tapered Element Oscillating Microbalance (TEOM) and Temperature Programmed Hydrogenation (TPH) under proper reaction conditions is used to quantify the various amounts of carbon deposits and Transmission Electron Microscopy (TEM) and magnetic measurements give indication on the state of the nickel phase along these processes. From these investigations, focussed on carbon deposits, the specificity of the hydrotalcite based system is outlined.

2. Experimental

2.1. Catalysts

The Ni/Mg(Al)O catalyst was prepared by synthesis of the corresponding hydrotalcite-like material with nominal composition $Mg_{5.88}Ni_{0.12}Al_2(OH)_{16}CO_3{\cdot}nH_2O$ and (Mg + Ni)/Al = 3.0, followed by calcination and reduction in a flow of

---

* Corresponding author. Tel.: +33 4 72 44 53 66; fax: +33 4 72 44 53 99.
E-mail address: mirodatos@catalyse.cnrs.fr (C. Mirodatos).

0920-5861/$ – see front matter © 2006 Elsevier B.V. All rights reserved.
doi:10.1016/j.cattod.2006.02.053

10 vol.% H_2/Ar, as reported in detail in ref. [4]. The BET surface area of the calcined material kept under inert conditions was 259 m^2/g for sieved fraction of grain size 0.2–0.3 mm [4]. The metal loading of Ni/Mg(Al)O was determined to be 1.8 wt.%.

Ni/SiO_2 was synthesized by calcining SiO_2-40 (Fluka, grain size 0.2–0.3 mm) at 825 °C for 10 h (giving a specific surface area of 164 m^2/g) before impregnating it with an aqueous solution of nickel nitrate. After impregnation, the product was dried overnight at 100 °C and calcined at 750 °C for 8 h in air. The metal loading was determined to be 1.8 wt.%. Ni/SiO_2 used for the TEOM (TPH) and magnetic measurements was activated (and then passivated) by a second heating to 650 °C in a fluidized bed reactor for 14 h in an atmosphere of 10 vol.% H_2/Ar, cooled to ambient temperature in the same atmosphere before the nickel metal surface finally was passivated by passing 2 vol.% O_2/N_2 over the material for 1 h. The specific surface area of the passivated Ni/SiO_2 catalyst was 100 m^2/g [5]. Ni/SiO_2 used in the stability tests were activated in a 10 vol.% H_2/Ar flow in situ at 650 °C for 14 h.

2.2. Catalytic reforming conditions

Long term activity and stability tests were performed in a quartz tubular reactor (i.d. 6 mm). The test temperature was measured with a thermocouple placed axially in the reactor inside a quartz thermocouple well (o.d. 3 mm). For Ni/SiO_2 and Ni/Mg(Al)O the catalytic bed height was 2.7 and 3.8 cm, respectively. The temperature gradient over the bed under reforming conditions was less than 2 °C. Duration times of the ageing tests were 8000–10,000 min (130–170 h), with a total gas flow rate of 55 N ml/min and with 0.45 g catalyst (WHSV = 7300 ml/h g_{cat}). Gas compositions (in vol.%) were: CH_4:CO_2:N_2 = 10:10:80 and C_3H_8:CO_2:H_2:N_2 = 10:30:10:50. When using propane as fuel, hydrogen was added to the feed to maintain the degree of Ni reduction and improve the catalyst performances.

The reactor effluent was analyzed by on-line gas chromatographic (GC) analysis (Agilent micro-GC equipped with three columns).

2.3. TEOM studies

Reaction, coke deposition, and regeneration by temperature programmed hydrogenation were carried out in a Rupprecht & Patashnick TEOM 1500 pulse mass analyzer. It consists of a microreactor with a high-resolution microbalance that generates real-time measurements of mass changes during gas–solid reactions [6–8]. The TEOM measures mass changes based on inertial forces, presenting key advantages over conventional gravimetric microbalances: (i) a well-defined flow profile, eliminating possible (heat and mass) diffusion and buoyancy phenomena, (ii) a very fast response time resolution (0.1 s), and (iii) a high mass resolution across the entire range of pressure and temperature.

The TEOM reactor was loaded with 72 mg of catalyst (sieve fraction 0.2–0.3 mm), firmly packed between two plugs of quartz wool. Prior to experiments the passivated catalysts were activated by a flow of 10 vol.% H_2/Ar using a ramp of 10 °C/min from room temperature up to 600 °C. When stable baseline was reached, Ar was replaced by the reaction mixture, and mass changes and product gases were continuously monitored. In addition to reaction mixture of 16 N ml/min, purge flow of 20 N ml/min (Ar) was used and the feed gases were preheated at 250 °C. The CH_4 and C_3H_8 reforming by CO_2 were carried out at 600 °C at a total pressure of $p = 1$ atm and a weight-hourly space velocity (WHSV) of 13,300 ml/h g_{cat}. Gas compositions (vol.%) were CH_4:CO_2:Ar = 10:10:80 and C_3H_8:CO_2:H_2:Ar = 10:30:10:50. The coke content was determined from the mass change measured during reaction, accounting for the mass change caused by the change of the gas density in the tapered element when Ar was replaced by the C_xH_y (+H_2) + CO_2 + Ar mixture.

The product gases were analysed by an on-line micro-GC (Quad SRA) equipped with a TCD, using Poraplot U and Molsieve 5A columns.

2.4. TPH experiments

TPH experiments were carried out on aged catalysts after cooling to room temperature under argon flow, then by ramping the temperature from 25 to 700 °C at 10 °C/min, under a flow of 5 vol.% H_2/Ar (50 N ml/min), following the outlet gas composition by mass spectrometry (mostly methane formation arising from the hydrogenation of carbon deposits).

2.5. Magnetic measurements

The amount of ferromagnetic Ni (giving access to the degree of Ni reduction) and the average metal particle size were determined for both catalysts, when activated, using the Weiss extraction method [9]. The sample (about 200 mg) was loaded in a specially designed fixed-bed reactor suited as sample holder in the electro-magnet. The passivated catalysts were heated to 600 °C (10 °C/min) in a flow of 10 vol.% H_2/Ar. Then the H_2/Ar mixture was switched to Ar, the cell was cooled to ambient temperature and sealed under an Ar atmosphere before collecting the magnetisation isotherms.

3. Results

3.1. Long term ageing tests

Figs. 1 and 2 report the activity/stability tests carried out over the Ni/SiO_2 reference catalyst and the Ni/Mg(Al)O hydrotalcite-derived catalyst both for dry methane and propane reforming to syngas at 600 °C and 1 atm.

For methane dry reforming over Ni/SiO_2 (Fig. 1), a fast deactivation occurs during the first minutes on stream followed by a slow and linear decrease in activity. For Ni/Mg(Al)O, a much improved stability is noted together with a higher CH_4 and CO_2 conversion.

For propane dry reforming (Fig. 2) a lower conversion than for methane is observed for both catalysts [e.g. 10% versus 30%

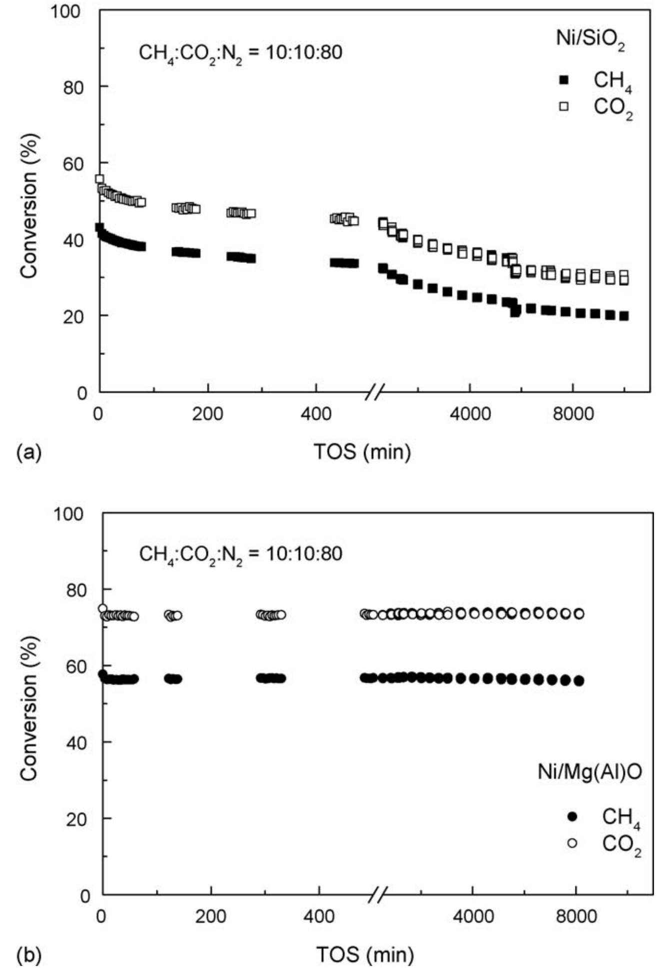

Fig. 1. Activity/stability tests at 600 °C for 8000–10,000 min (130–170 h) under a CH_4:CO_2:N_2 = 10:10:80 stream. (a) Ni/SiO_2 and (b) Ni/Mg(Al)O.

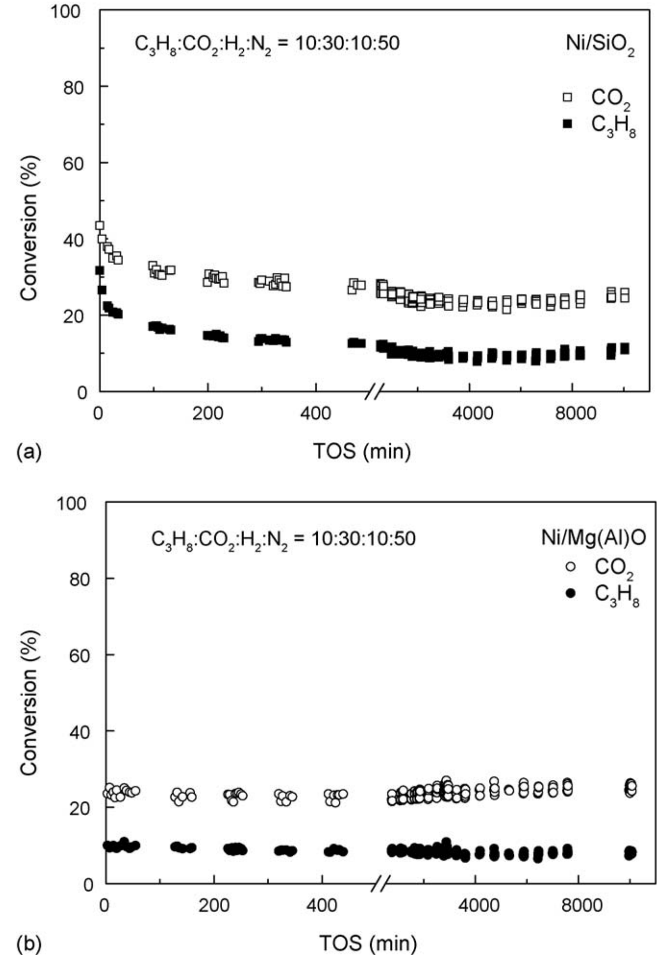

Fig. 2. Activity/stability tests at 600 °C for 10,000 min (170 h) under a C_3H_8:CO_2:H_2:N_2 = 10:30:10:50 stream. (a) Ni/SiO_2 and (b) Ni/Mg(Al)O.

hydrocarbon conversion after 6000 min (100 h) over the reference catalyst]. For Ni/SiO_2, an initial deactivation is observed followed by a stable conversion, while the Ni/Mg(Al)O system remains perfectly stable over the run. In ref. [4], a stability test lasting for 34 days showed the same features.

3.2. Catalytic tests in the TEOM reactor

Methane and propane dry reforming experiments carried out in the TEOM reactor are reported in Fig. 3 (methane reforming) and Fig. 4 (propane reforming).

The deactivation curves recorded both for methane (Fig. 3A) and propane (Fig. 4A) in the TEOM reactor reflect well the trends reported above for long term ageing experiments in fixed bed reactor (Figs. 1 and 2), even though slight differences in performances are noted, likely due to the difference in reactor configuration (WHSV, geometry, catalyst bed packing, etc.). Main findings are: (i) in all cases the CO_2 conversion is higher than that for methane or propane (due to RWGS), (ii) for both hydrocarbons, the deactivation is less pronounced for hydrotalcite based material, the difference being largest for methane dry reforming, and (iii) both for methane and propane dry reforming, the stabilized or pseudo stabilized conversion (after an initial deactivation within the first 2 h on stream) is about two times higher for the hydrotalcite based system than for the Ni/SiO_2 one.

3.3. Changes in mass

Mass changes observed in data presented in Figs. 3B and 4B can unambiguously be assigned to carbon deposits, since the eventual contribution of the supports (e.g. hydroxylation and/or carbonatisation of silica or hydrotalcite Mg(Al)O materials) have been accounted for from blank experiments. The main trends observed are: (i) for both types of catalysts, a fast initial carbon uptake is noted either for methane or for propane dry reforming, which corresponds to the initial deactivation reported above. This carbon uptake during the initial period is about 2.5–4 times larger for Ni/SiO_2 than for Ni/Mg(Al)O and about 1.5–2 times larger for propane than for methane reforming (0.5 wt.% versus 0.13 wt.% for methane reforming and 0.8 wt.% versus 0.3 wt.% for propane reforming), (ii) after this initial period, the rate of carbon uptake (slope of the mass curve) remains about three times lower for Ni/Mg(Al)O than for Ni/SiO_2 (below 0.01 wt.% h^{-1} versus 0.03 wt.% h^{-1} both for methane and propane reforming). It was even noted that

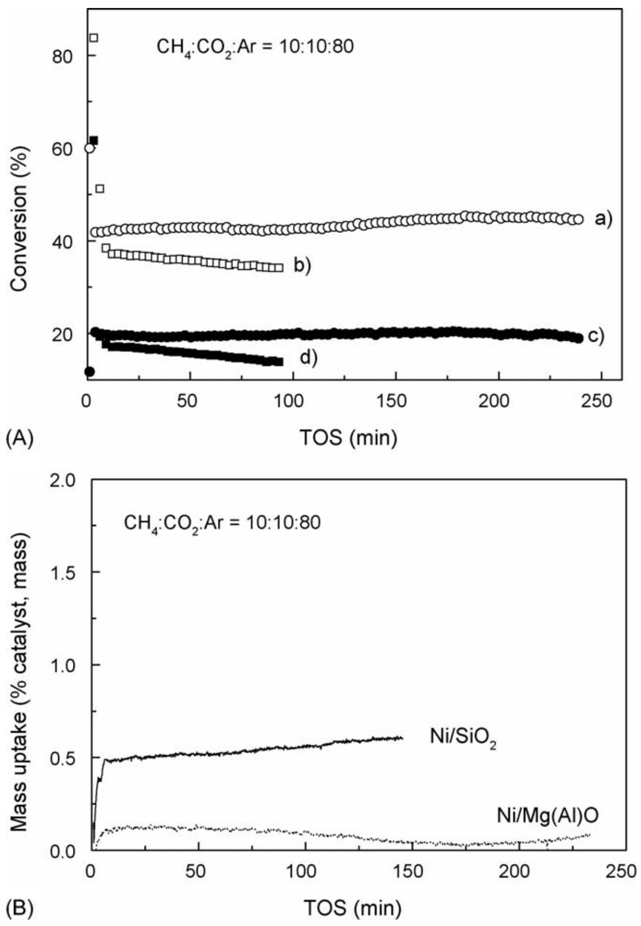

Fig. 3. (A) Changes in methane [(●) (c), (■) (d)] and carbon dioxide [(○) (a), (□) (b)] conversion vs. time on stream (min) in the TEOM reactor over Ni/SiO$_2$ [(□) (b), (■) (d)] and Ni/Mg(Al)O [(○) (a), (●) (c)]; (B) Mass uptake (expressed as carbon wt.% referring to the catalyst) vs. time on stream (min) for methane dry reforming in the TEOM reactor for Ni/SiO$_2$ and Ni/Mg(Al)O.

some transient loss in mass could occur for methane reforming over Ni/Mg(Al)O (Fig. 3B).

3.4. TPH experiments

TPH experiments were carried out after various times on TEOM stream, as illustrated in Figs. 5 and 6 for the hydrotalcite based system and in Fig. 7 for comparing Ni/SiO$_2$ and Ni/Mg(Al)O systems after propane dry reforming.

As can be seen for the hydrotalcite based system, either for methane (Fig. 5) or propane (Fig. 6) dry reforming, two main types of carbon are formed upon time on stream; (i) a small amount accumulating within the first 0.1 h on stream, which can be hydrogenated between 200 and 500 °C, and which does not further evolve for longer ageing period, and (ii) a more abundant and stable carbon, which can be hydrogenated only at around 600 °C, and which slowly and regularly accumulates with time on stream. It can be noted also in Fig. 6 that the amount of stable carbon accumulating with time on stream is higher for propane than for methane reforming, in agreement with the TEOM results.

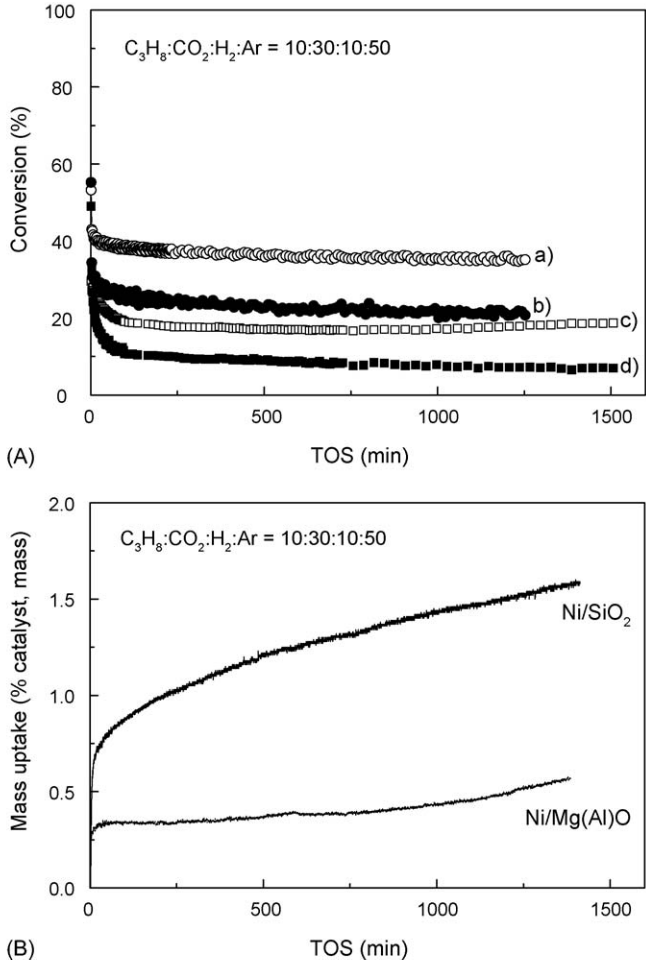

Fig. 4. (A) Changes in propane [(●) (b), (■) (d)] and carbon dioxide [(○) (a), (□) (c)] conversion vs. time on stream (min) in the TEOM reactor over Ni/SiO$_2$ [(□) (c), (■) (d)] and Ni/Mg(Al)O [(○) (a), (●) (b)] catalysts; (B) Mass uptake (expressed as carbon wt.% referring to the catalyst) vs. time on stream (min) for propane dry reforming in the TEOM reactor for Ni/SiO$_2$ and Ni/Mg(Al)O.

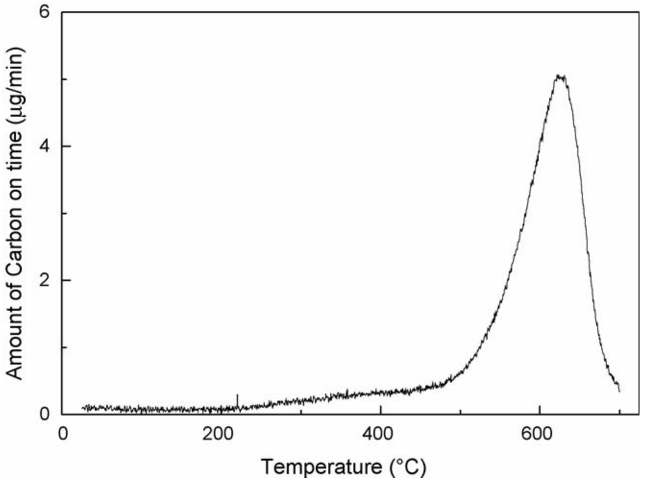

Fig. 5. Amount of carbon hydrogenated into methane during TPH experiments after TEOM methane dry reforming over Ni/Mg(Al)O for 4 h. Heating rate during the TPH experiment was 10 °C/min.

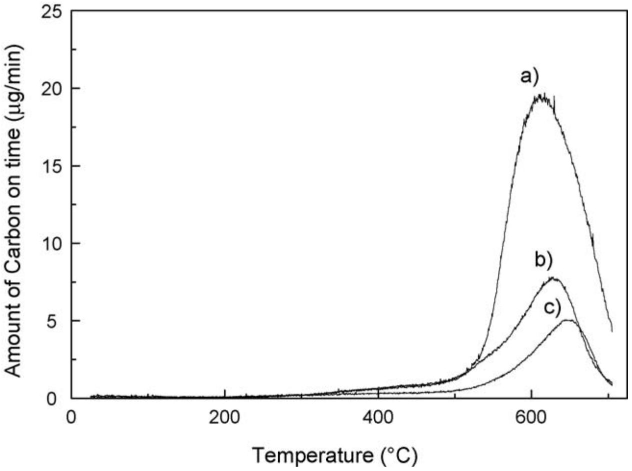

Fig. 6. Amount of carbon hydrogenated into methane during TPH experiments after TEOM propane dry reforming over Ni/Mg(Al)O for 0.1 h (b) and 24 h (a). For comparison, curve (c) is similar to one curve in Fig. 5 (related to methane dry reforming). Heating rate during the TPH experiment was 10 °C/min.

For Ni/SiO_2 reference catalysts, similar trends were already reported for methane dry reforming [1]. For propane dry reforming over Ni/SiO_2 (Fig. 7), it can be noted that the more reactive carbon can be hydrogenated at lower temperature than for the hydrotalcite based material.

3.5. TEM analyses

From TEM analyses reported in ref. [1] it was observed for Ni/SiO_2 that most of the Ni particles after reduction had a size comprised between 4 and 8 nm. For Ni/Mg(Al)O [4], most of the particles were below 5 nm, while some large particles were observed in the range 20–40 nm. After methane dry reforming tests, it was noted that for Ni/SiO_2, both two-dimensional carbon veils and whiskers accumulate upon time on stream, with a large number of Ni particles being located on top or at the intersection of carbon whiskers. In contrast, whiskers growth was only scarcely observed for the hydrotalcite based system.

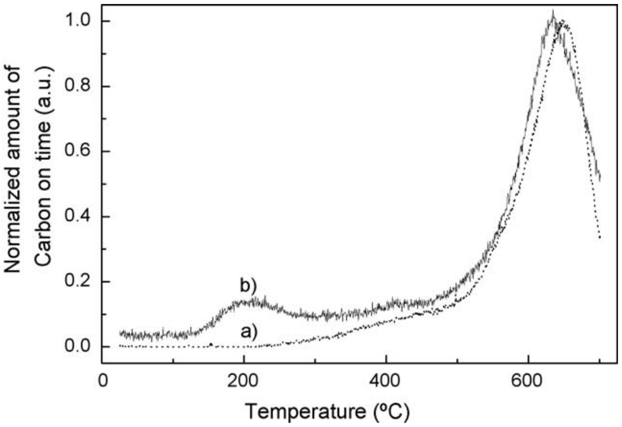

Fig. 7. Normalized amount of carbon hydrogenated into methane during TPH experiments after TEOM propane dry reforming for approximately 0.1 h over Ni/Mg(Al)O (a) and Ni/SiO_2 (b). Heating rate during the TPH experiment was 10 °C/min.

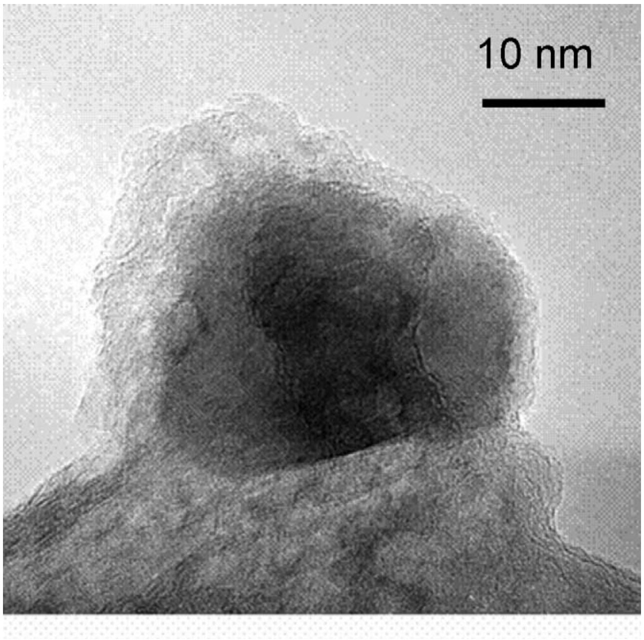

Fig. 8. TEM image of a large Ni particle after 12 h under propane dry reforming stream over 1.9 wt.% Ni/Mg(Al)O [4].

Only bidimensional carbon layers or veils around the Ni particles and on the support were observed, and the Ni particles remaining embedded into the support, as depicted for a large particle in Fig. 8 [4]. Note that the main fraction of small particles (below 5 nm) was still on the support, though the presence of carbon hindered a precise evaluation of their mean size [4].

3.6. State of the nickel phase from magnetic measurements

Table 1 summarizes data obtained from magnetic measurements after the reduction. As can be seen, the hydrotalcite based material is much less reduced than Ni/SiO_2, with a better dispersion of the metallic phase (in agreement with the above TEM data), as expected from the strong metal support interaction typical of this material [4]. Some magnetic measurements, not reported here [10], were also recorded after catalytic tests. They indicate a trend to some decrease in the ferromagnetic content, especially for the Ni/SiO_2 system. Such a trend may indicate a transformation of part of the metallic Ni phase (ferromagnetic) into nickel carbide (non-ferromagnetic) or with interstitial carbon within the Ni phase (less ferromagnetic). For the hydrotalcite system, it was even

Table 1
Nickel phase characterization data from magnetic measurements

Catalyst treatment	Degree of Ni reduction (%)		Mean particle size (nm)	
	Ni/SiO_2	Ni/Mg(Al)O	Ni/SiO_2	Ni/Mg(Al)O
After reduction at 600 °C	≈95	≈20	8	5–6[a]

[a] This mean value, due to the very low amount of ferromagnetic signal, does not exclude that large particles may also coexist, like the one observed by TEM in Fig. 8.

observed in some cases a slight increase of the ferromagnetic content, which here could suggest a further reduction of the Ni phase under reforming conditions.

4. Discussion

4.1. Nature of the ageing process

By checking that the degree of Ni reduction and the mean particle sizes do not change in a significant way along the reforming runs (either for methane or propane) [10], it can be deduced that for the present investigation, most of the catalyst ageing, reflected by the loss of activity, is due to carbon deposits. Note however that in the presence of real natural gas feed, other sources of poisoning such as sulphur deposits should be accounted for, in addition to coke poisoning.

4.2. Nature of carbon deposits

From TEOM, TPH and TEM experiments, it was observed that at least two types of carbon deposits are formed during the dry reforming processes: (i) carbon deposits accumulating within the first minutes on stream, which can be hydrogenated between 200 and 500 °C, and which does not further evolve for longer ageing period (denoted as low temperature carbon, C_{LT}), and (ii) a more abundant and stable carbon, which can be hydrogenated at around 600 °C, but which slowly and regularly accumulates with time on stream (denoted as high temperature carbon, C_{HT}).

(i) C_{LT} cannot be considered as long term deactivating carbon, since it is rapidly accumulating and stabilizing as soon as the reduced catalysts are contacted with the reacting feed. It was already assigned, for the case of methane dry reforming on Ni catalysts, to a combination of Ni surface and bulk carbon species, which play a direct role in the reforming mechanism. Its concentration was shown to depend on the reaction conditions and the reactivity of the Ni phase, as a function of metal loading, addition of dopants like alkali or alkaline earth elements, nature of the support, etc. [1]. By dividing the molar amount of these active carbon deposits by the molar amount of surface nickel (deduced from the mean Ni particle size), the ratio $C_{LT}/Ni_{surface}$ can be evaluated, as reported in Table 2 for the various studied cases.

Within the uncertainties in the experimental methods for calculating this ratio, it could be first underlined that the concentration of this active carbon leading to CO formation seems to be slightly more abundant for Ni/Mg(Al)O than for Ni/SiO_2, and for methane than for propane reforming. On a more quantitative point of view, by considering these $C_{LT}/Ni_{surface}$ values in Table 2, it can be speculated that this active carbon C_{LT} would correspond to NiC, Ni_2C or Ni_3C surface carbon (nickel carbide like), as already reported in the literature for methane steam or dry reforming [1].

Table 2
Values of the $C_{LT}/Ni_{surface}$ as deduced from TPH and TEOM measurements

Catalysts	Ni/SiO_2	Ni/Mg(Al)O
Methane dry reforming	0.3[a]	1.8
Propane dry reforming	0.2	1.1

[a] From ref. [1].

(ii) At variance with C_{LT}, C_{HT} seems to directly control the long term deactivation process. Thus, for Ni/SiO_2, the regular rate of deactivation appears to correspond to the regular accumulation of C_{HT}, while for Ni/Mg(Al)O, the low rate of stable carbon uptake seems to ensure the long term catalyst stability. However, from the TEM analyses, it is concluded that this C_{HT} comprises most likely at least two forms of graphitic carbon; the whiskers observed only for Ni/SiO_2 and the bidimensional carbon observed both for Ni/SiO_2 and Ni/Mg(Al)O.

Specificities of the hydrotalcite based system as compared to the reference Ni/SiO_2 catalyst: From the above observations, it was shown that on both catalytic systems, the dry reforming of methane or propane is likely to proceed via similar active surface carbide like intermediates, though the ratio C_{LT}/Ni revealed some slight differences depending on the catalyst and on the reformed hydrocarbon.

In contrast, major differences were revealed for the two studied catalytic systems concerning the stable and accumulating carbon and the kinetics of accumulation:

- On *the reference silica based system*, the carbon deposition has been well described elsewhere [1]. It combines (i) the formation of carbon nanotubes by carbon extrusion from dense planes, favoured by the fact that the Ni particle are not fixed on the silica and can be transported by the nanotubes and (ii) encapsulating carbon which progressively limits the access of the reacting gases to the active surface. The carbon whiskers cannot be considered as participating to the catalyst ageing, unless random and side phenomena like particle fragmentation take place (due to surface and bulk constraints (Ni carbide) and further on to pores and reactor plugging). In contrast, the bidimensional form of encapsulating carbon, rather favoured by the free access to all sides of the particles, unambiguously leads to catalysts deactivation. From this analysis, the curves of carbon uptake for Ni/SiO_2 (Fig. 4B) can be interpreted as such: initial fast surface carbide build-up followed by the regular accumulation of both carbon nanotubes (not toxic unless large amounts deposited) and encapsulating deactivating carbon.
- For the *hydrotalcite based system*, the strong metal/support interaction which embeds the Ni particles onto the support hinders the formation of carbon nanotubes, since only part of the particles' surface is accessible to the reacting gases, which prevents any extrusion from the other side. Such a configuration also hinders the formation of encapsulating layers around the particles, which is proved by the low amount of C_{HT} detected by TPH. Though outside the scope of the present paper, a full investigation comparing the mechanism of methane and propane dry reforming (to be published) also indicates that the hydrotalcite support plays another major role which is to provide continuously oxygen to the Ni surface and which obviously limits the formation of

any toxic carbon around the particles. The source of oxygen is ensured by a pool of carbonates around the Ni particles (well identified from in situ DRIFT spectra not reported here) able to decompose into CO and surface oxygen.

4.3. Specificities of methane and propane dry reforming

As seen by comparing Figs. 3B and 4B and in Table 2, it is concluded that methane dry reforming tends to produce significantly less surface and out-of-surface carbon than propane dry reforming. This trend should still be reinforced by performing the propane dry reforming experiments in the absence of added hydrogen in the feed. For surface carbon, it can easily be understood that the cracking of methane into surface carbon as a preliminary step involves only C–H bond breaking, while C–C bonds are also involved for propane reforming. Therefore, it can be speculated that: (i) for methane reforming, the probability to form C–C bonds as coke precursors from the atomic carbon species (easily formed from methane cracking) is low due to the fast competitive oxidation by surface oxygen provided by CO_2 dissociation, and (ii) for propane reforming, the probability to form coke precursors is much higher since C_3 partially dehydrogenated adspecies may easily form and polymerise into polyaromatics, in competition with the CO formation. This process might involve a transient formation of propylene as assumed in ref. [2]. Further differences between the two reforming mechanisms will be reported in a forthcoming study.

5. Conclusions

From the preliminary data presented in this paper, combined with data already published or still to be published, major differences were observed by comparing two nickel based catalysts for the dry reforming of methane and propane. The much higher stability of the hydrotalcite based system was assigned (i) to the morphology and structure of the nickel phase, remaining in strong interaction with the support under reaction conditions, while the Ni particles are easily extracted from the silica surface, and (ii) to an active role of the hydrotalcite support which is to provide continuously oxygen to the nickel surface. It was also demonstrated that methane reforming generates less surface and out-of-surface carbon than propane reforming. This might be related to the competition between the initial steps of cracking, polymerization and carbon oxidation, highly sensitive to the nature and structure of the molecules to be reformed.

References

[1] L. Pinaeva, Y. Schuurman, C. Mirodatos, in: M. Maroto-Valer, C. Song, Y. Soong (Eds.), Environmental Challenges and Greenhouse Gas Control for Fossil Fuel Utilization in the 21st Century, Kluwer Academic/Plenum Publishers, 2002, p. 313.
[2] F. Solymosi, P. Tolmacsov, K. Kedves, J. Catal. 216 (1–2) (2003) 377.
[3] D. Sutton, J.F. Moisan, J.R.H. Ross, Catal. Lett. 75 (2001) 175.
[4] A. Olafsen, Å. Slagtern, I.M. Dahl, U. Olsbye, Y. Schuurman, C. Mirodatos, J. Catal. 229 (2005) 163.
[5] M.B. Jensen, U. Olsbye, A. Olafsen, G. Ghiotti, in preparation.
[6] D. Chen, H.P. Rebo, K. Moljord, A. Holmen, Chem. Eng. Sci. 51 (1996) 2687.
[7] W. Zhu, J.M. van de Graaf, L.J.P. van den Broeke, F. Kapteijn, J.A. Moulijn, Ind. Eng. Chem. Res. 37 (1998) 1934.
[8] S.A. Gembicki, K.M. VandenBussche, A.R. Oroskar, Chem. Eng. Sci. 58 (2003) 549.
[9] J.A. Dalmon, in: Boris Imelik, Jacques C. Védrine (Eds.), Catalyst Characterization, Plenum Press, New York, 1994, p. 585.
[10] L.B. Raaberg, A. Olafsen, M.B. Jensen, C. Daniel, C. Mirodatos, U. Olsbye, in preparation.